Critical Design Review
Data Package Document 1

CubeSat Design Overview Report

CubeSat Design Overview Report

Table of Contents

CubeSat Design Overview Report

1. System Overview

This document outlines the detailed design review of the i-INSPIRE II CubeSat for QB50. During the mission lifetime we will demonstrate innovative space technologies developed by the University of Sydney. The technologies include an improved space photonic device for remote sensing, a FPGA-based controller for OBDH and ADCS. Also a camera will be integrated for taking images of the Earth and other QB50 satellites; and a radiation counter will be used for recording the level of radiation. The i-INSPIRE II satellite bus is developed using commercial-off-the-shelf parts. The satellite equips a 30 Wh power board with an intelligent power management controller. We are using the solar panels from ClydeSpace. Although we will demonstrate the FPGA for OBDH, the main on-board computer will be a low power MSP430 controller. The satellite will be controlled using magnetic torque from ClydeSpace. We will also use our novel reaction wheel to control the rotation of Z-axis. The attitude determination system includes a MEMS IMU and sun sensors. The satellite will use VHF for uplink at 1200bps and UHF for downlink at 9600bps. A GPS is used to determine the location of the satellites.

Fig. 1 shows the diagram for the i-INSPIRE II cubesat design. And Table 1 list the components of the subsystems, where it clarifies whether we are using COTS components or designing in-house.

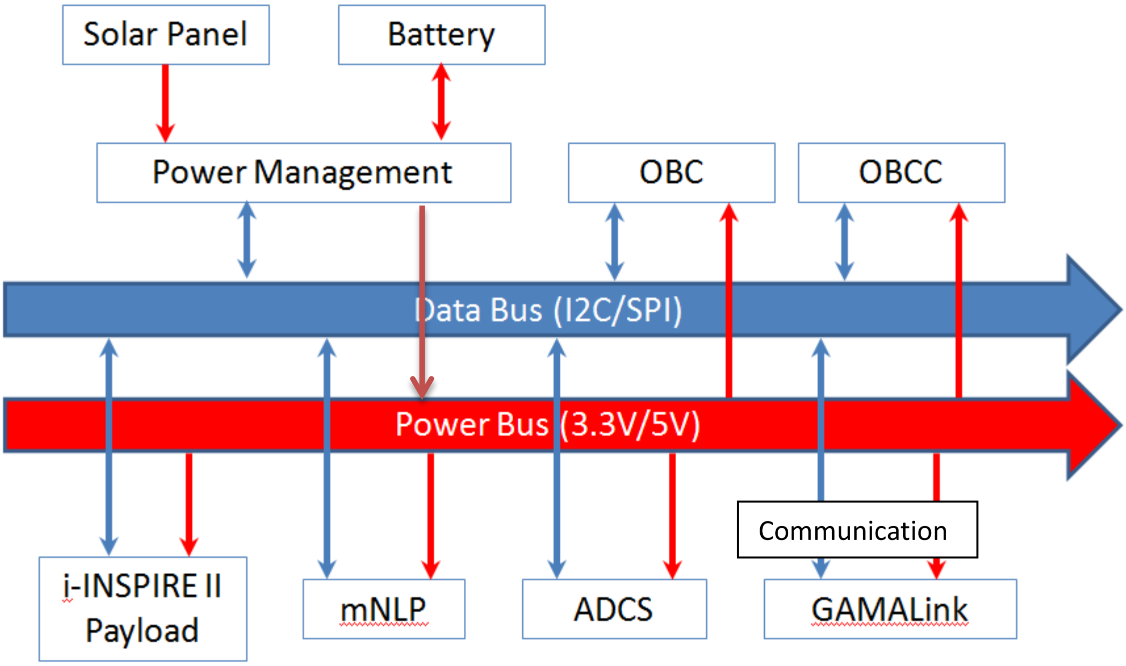

Fig. 1. i-INSPIRE II cubesat design diagram

Figure 2 presents an exploded view of the i-INSPIRE II.

Table 1: List of the components

Subsystem	Description/Vendor	TRL/Part No.
Structural	In-house design using AL7075	TRL 5
Solar Panel	1 front panel with magnetorquer, and 1 front panel, Clyde-Space	SP-L-S2U-0031-CS-MGT
	1 side panel with magnetorquer, and 1 side panel, Clyde-Space	SP-L-F2U-0033-CS-MGT
actuators	1 reaction wheel (designed in house)	TRL 6
	3 magnetorquers from Clyde-Space: two are integrated with solar panels; one is standalone	17.01 (for standalone magnetorquer)
Attitude sensor	1 IMU stick from Sparkfun	SEN-10724
	6 Sun sensors from TAOS	TSL260R-LF
Battery	6 LiPoly batteries from Varta	LPP454261 8TH
EPS	In-house design	TRL 5
OBC	MSP430F5438 from Olimex	MSP430-H5438
OBCC	Xilinx Spartan 6 FPGA board from Enterpoint	XC6SLX150 X1
TT&C	GAMALink	TRL5
TT&C	ISIS trasceiver	TRX-VU
Thermal	In-house design	TRL 5
i-INSPIRE II payload	Camera/earth sensor from Sparkfun	SEN-11610
	In-house designed radiation counter	TRL 6
	In-house designed NanoSpec	TRL 6

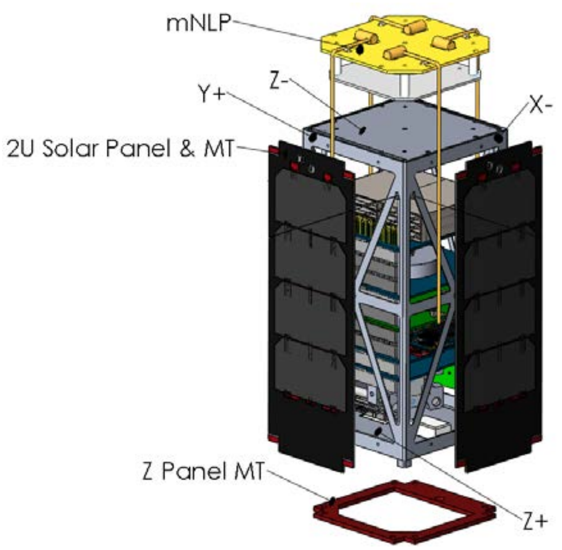

Fig. 2. Overview of the i-INSPIRE II satellite.

2. Payload Design

The i-INSPIRE II will accommodate the mNLP sensor set for the common QB50 mission. At the same time it will carry three scientific instruments to fulfill the observation in orbit. Except the imager which is the COTS device, NanoSpec and radiation counter are designed in house. Furthermore, the drivers for each instrument are designed and implemented on the MSP430 processor. Fig. 3 shows our payload board for the i-INSPIRE I mission.

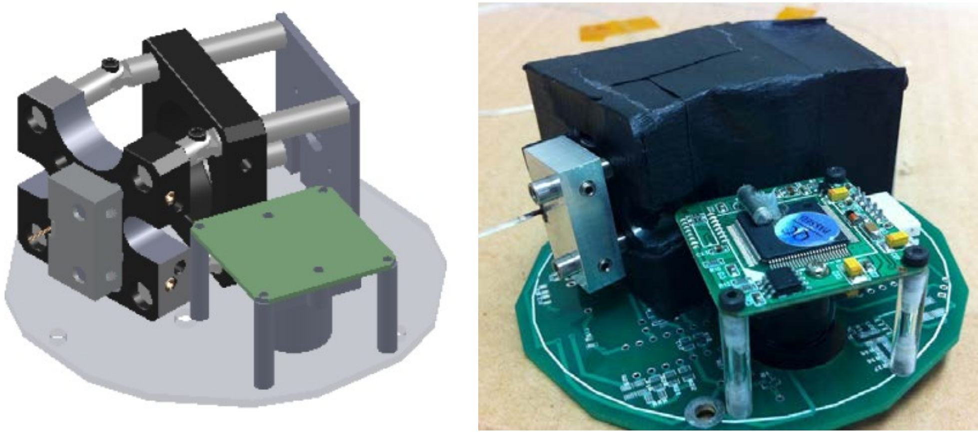

Fig. 3. CAD model of payload board and practical integration of payloads

Imager

The imager used in the i-INSPIRE II is one COTS version from the Sparkfun as shown in Fig. 4. The resolution can be chosen from VGA, QVGA or 160x120 in software. The optical sensor on this imager can automatically compress the image into JPEG format. As one CMOS instrument, however, this imager is still need the 5V power supply to guarantee the normal operation. According to the measurement from multi-meter, the current consumption is about 90mA. Because communication window with ground station is relatively narrow which is estimated about 5 minutes, the amount of transmitted data in downlink is approximately equal to 32KBytes. Therefore, the resolution of image is set in 160x120 with picture size of only 4KByte.

Fig. 4. JPEG Color imager used in i-INSPIRE II

Nano-spectrometer

This instrument (shown in Fig. 5) is developed by School of Physics in University of Sydney. The goal of NanoSpec is to demonstrate the potential of photonics-driven technology in space-based applications. The Nano-spectrometer is designed and built as one single mode fibre-fed diffraction limited device, which will survive a launch into space while still providing a reasonable spectral resolution. The spectrograph design is based upon the relatively simple PIMMS (Photonic Integrated Multimode MicroSpectrograph) type device, which is effectively independent of its light source.

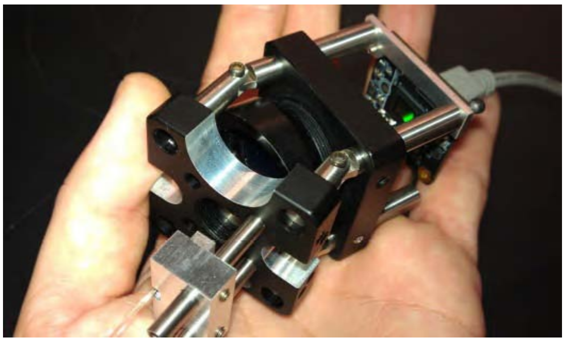

Fig. 5. Photonic spectrograph used in i-INSPIRE satellite

NanoSpec is a diffraction limited single-mode fibre (SMF) fed spectrograph based upon the PIMMS concept described by Bland-Hawthorn el al. in 2010 [1]. The concept is inspired by the efficient multi-mode to single-mode conversion of the photonic lantern [2–4]. These allow for a spectrograph to be fed light by an array of SMF. Given the fundamental form of propagation in SMF, this is equivalent to smallest possible input slit that can be used on a spectrograph (it is diffraction limited). Consequently, the spectrograph resolving power becomes dependant purely on the dispersing element, namely the number of lines illuminated on the diffraction grating. Additionally, it allows for the an extremely compact design and reduces complexities in alignment and construction, making it suitable for use in a small satellite.

Current implemented design has eight single mode fibres and the arrangement is shown as Fig. 5. This arrangement is aimed to ensure that regardless of the attitude of satellite, a spectrum will be generated by astronomical sources such as the Sun and Moon. There are two different types of optical fibre used in NanoSpec, which are represented by red and blue lines in Fig. 6. One is a typical step index fibre where light guiding is achieved via a higher refractive index in the core of the fibre than the cladding. The second is a photonic crystal fibre where light is guided by a pattern of air filled holes in the core of a silica fibre. The performance of pairs of fibres will be tested in LEO environment.

In order to satisfy both the cost the size and cost constraints, the spectrograph will operate in the visible (~400-750nm). The performance of COTS achromatic lenses reduces this to a wavelength range 450- 700nm. The COTS detector used currently is of the VGA (640x480) format with 6µm pixels.

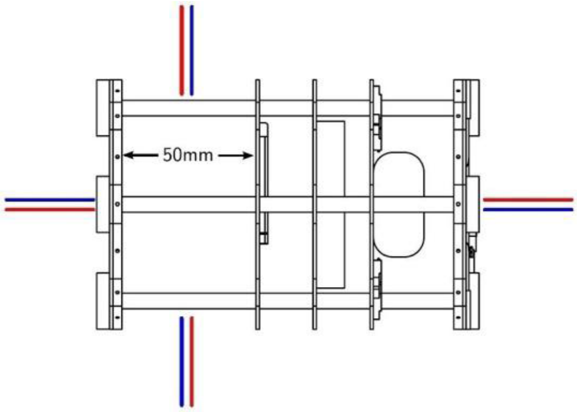

Fig. 6. Fibres arrangement in a side view

The actual operation of NanoSpec is simpler unlike its complex structure. Since it uses the COTS imaging detector, the operation procedures are similar to imager. The MSP430 sends the commands and make the NanoSpec collect spectrogram. And then, the spectrogram in JPEG will be retrieved and stored into micro SD card.

Radiation counter

During the flying in orbit, the single event upset (SEU) is harmful for onboard electronic devices. To detect the radiation level during the flying in orbit, one radiation (Geiger) counter is carried by satellite.

Fig. 7 shows the body of miniaturized radiation counter. The integrated black module is a powerful transformer from EMCO. To guarantee the survival in the hazard space environment, the solid capacitors are used. The radiation counter uses one NE555 timer which will generate a clock pulse when it is triggered by every tailing edge from radiation tube.

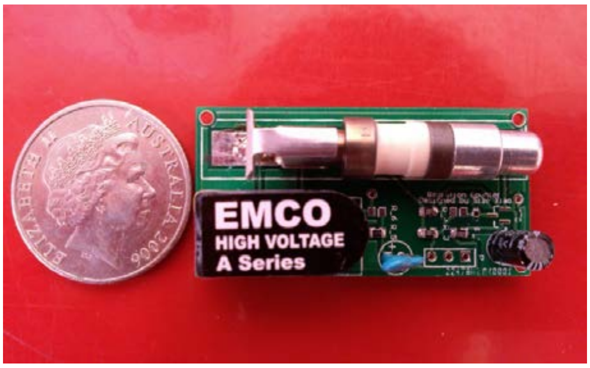

Fig. 7. Proposed Geiger counter comparing with Australian twenty-cent coin

The EMCO high-voltage power supply has enough internal protection mechanisms, including an internal softening resistor and pulse-by-pulse current limiting, to adequately deal with high voltage output short-to-ground faults. A basic scheme to protect other electronic system from the high voltage out is using high voltage electrical insulating tape. However, to prevent the arcing problems, high-voltage-power-supply grounding schemes are designed to assuring proper performance and reliability. Each ground should be connected via a dedicated grounding wire.

The Geiger tube is a commercial-off-the-shelf product from LND Inc. This tube is made of a thin-walled stainless steel and is filled with a mixture of Neon and Halogen gases at low-pressure.

On the other hand, the drawback of miniaturization should be clarified. We pay for the decline in detector sensitivity as the cost. The sensitivity is depending on the volume of the radiation tube (detector), or the pressure of the gas filled in the tube, and the voltage as well. One Geiger tube with higher voltage is more likely to generate a pulse when a particle goes through. Taking everything into account, this miniaturized design is not perfect for its performance but could be the appropriate one for our mission. With the help of radiation source---Co-60, the single radiation event can be displayed on oscilloscope as shown in Fig. 8.

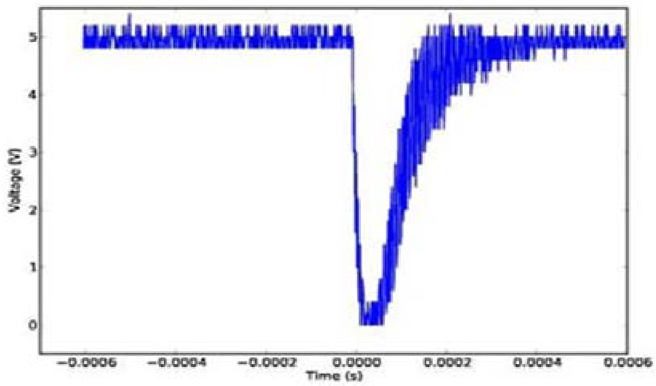

Fig. 8. Output pulse from designed Radiation counter

The operation for radiation counter is not complex in software. Its output is designed to be compatible with TTL standard. Any radiation event will cause one pulse on main processor's I/O and relevant trailing edge will trigger the interrupt on main processor. In the interrupt routine, it will record the amount of coming events and the result of record will be stored as individual files periodically.

Functionally, current design of radiation counter is qualified for i-INSPIRE mission. On the other hand, some issues regarding compatibility with other components need to be addressed. The radiation detector (tube) should work with 584V high voltage which could cause the breakdown and damage other devices since the payload space is crowded. High voltage insulation tape will be used to guarantee the safety of whole system.

Data budget

We assume the zenith facing field of view (FOV) of the ground station is between 160 – 170 degrees. The amount of data transmittable in one day assuming a data rate of 9.6 kbps is given in the table below for different FOV angles and the QB50 operation altitudes of 200 km – 350 km. Calculations were performed on both Satellite Tool Kit (STK) and via a MATLAB simulation.

Table 2: Data allowed transmitting in 1 day

Data in 1 day assuming given rate [Mb]						
FOV x Alt	**200 km**	**230 km**	**260 km**	**290 km**	**320 km**	**350 km**
160 deg.	2.75	3.11	3.96	4.69	5.36	6.03
170 deg.	5.06	6.04	7.07	8.12	9.11	10.1
180 deg.	10.14	11.51	13.07	14.50	16.02	17.37

From the table we can see that even at 200 km, the satellite safely guarantees > 2 Mb of data/day, providing 38% more data than required by QB50 specifications. We show that even with the 160 deg. FOV, the total satellite data budget is within limits dictated by access times. (We envisage that a FOV closer to 170 deg. to be more accurate as a wide FOV omnidirectional turnstile antenna will be used in conjunction with the high gain Yagi-Uda tracking antenna).

The data rate for downlink is 9600 bps using BPSK and AX.25. If we assume the minimum overhead is 18 bytes for AX.25 packets, for each second the effective data transmittable is 1182 bytes; or 98.5% of the data specified in the table above, for scientific return per day. Apart from the QB50 sensor data, we expect to transmit housekeeping, image, radiation and NanoSpec data, similar to the i-INSPIRE I satellite. The data budget for the i-INSPIRE II is shown in the following table.

We see that the data budget is met even for the satellite at 200 km with a 160 deg. FOV of the ground station. All higher altitudes and greater FOVs (which we expect for most of the operation of the satellite) result in a higher data rate significantly above what is required as the basic requirement.

Table 3: Maximum data for transmission in the worst scenario

WORST SCENARIO			
FOR QB50			
Data Budget (FOV = 160 deg., Altitude = 200 km) worst case			
downlink data rate (kb/s)	9.6		
Downlink time in one day (s)	285.984		
Data transfer in one day (kb)	2745.4464		
	Unit data [kb]	Number of units acquired in one day	Total Data [kb]
Single spectra from NanoSpec (752*16 Bytes)	94	4	376
Radiation counter data	0.032	1440	46.08
Single Colour Image (JPG90- VGA)	48	4	192
		Total data for our own sensors [kb]:	**614.08**
		Data available for QB50 sensors [kb]:	**2131.3664**
BEST FOV SCENARIO AT 200 km Altitude			
FOR QB50			
Data Budget (FOV = 180 deg., Altitude = 200 km)			
downlink data rate (kb/s)	9.6		
Downlink time in one day (s)	1056.672		
Data transfer in one day (kb)	10144.0512		
	Unit data [kb]	Number of units acquired in one day	Total Data [kb]
Single spectra from NanoSpec (752*16 Bytes)	94	56	5264
Radiation counter data	0.032	1440	46.08
Single Colour Image (JPG90- VGA)	48	56	2688
		Total data for our own sensors [kb]:	**7998.08**
		Data available for QB50 sensors [kb]:	**2145.9712**

3. Structural Subsystem

The Structural subsystem of the I-INSPIRE II will use in house design for providing better compatibility. Apart from following the structural subsystem requirements of QB50 project strictly, the design will also focus on: locate the centre of gravity at around the geometric centre; make mass distribution as symmetric as possible, provide the onboard subsystems the required field of view; minimise the CubeSat product of inertias, optimise the layout of electrically linked components to reduce cabling; ease to manufacture and assemble.

The structure of the I-INSPIRE II will be designed base on bent sheet metals, this concept will be able to maximise accommodation for onboard components and minimise the structural weight. The structure of the I-INSPIRE II is depicted in Fig. 9. Detailed assembly procedures will be included in Document 3 “Assembly, Integration and Test Plan”.

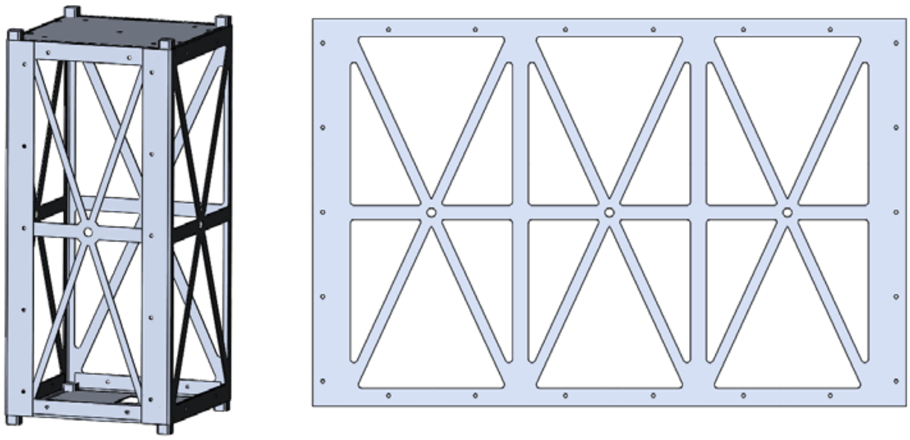

Fig. 9. Structure of I-INSPIRE II

By considering the strength, weight, manufacturability and weight, Aluminium 6061 is chosen for the primary and secondary structures of I-INSPIRE II. Compare to some of the other similar materials, Aluminium 6061 has higher strength and workability, beside; it’s fully compatible with the material of the P-POD.

Two hatches as required by the QB50 are located at the bottom plate. These two hatches will provide access to the on-board computers using two connectors. The two connectors as shown in Fig. 10 have a number of head pins which are configured as two JTAG ports and two USB ports to program and debug the MSP430 microcontroller and the Spartan 6 FPGA. At the same time, the external power supply will also be provided to the satellite through the connectors. The dimension of the two connectors is 13mm x 25mm and 13mm x 19mm respectively.

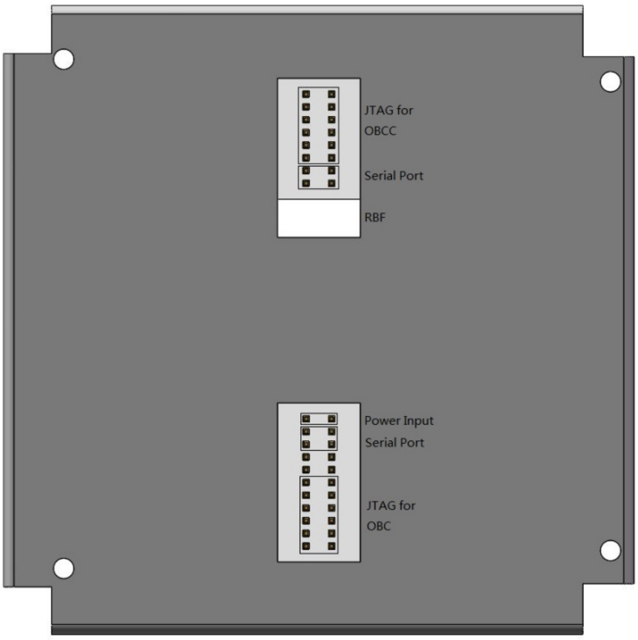

Fig. 10. The two connectors.

The Finite Element Analysis

The finite element analysis has been conducted in Solidworks, the structure was examined to simulate the worst load case scenarios in acceleration, vibration and shock. All simulation profiles were obtained from the QB50 System Requirements.

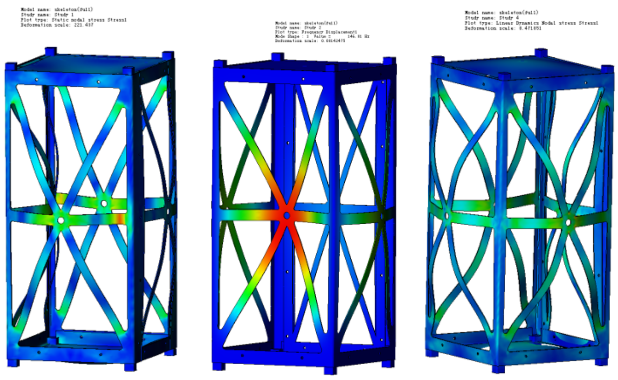

Fig. 11. FEA analysis of I-INSPIRE II structure

In acceleration test, the quasi-static loads are 12g in all directions, the simulation result in Fig. 11 shows that the factor of safety is 21. It demonstrates the over-designed nature of the structure and should ensure a reliable platform. The payload of the launch vehicle has to be designed with a structural stiffness which guarantees that there is not resonance will exist, therefore the natural frequencies from simulation must be above the constraint value (90Hz) from QB50 design requirement. The modal analysis shows that the first mode of the structure is 145 Hz and it is acceptable. In random vibration test, using the vibration test characteristics provided by the design requirement, it shows that the von-Mises stress are under safety range as shown in Fig. 12 a and b.

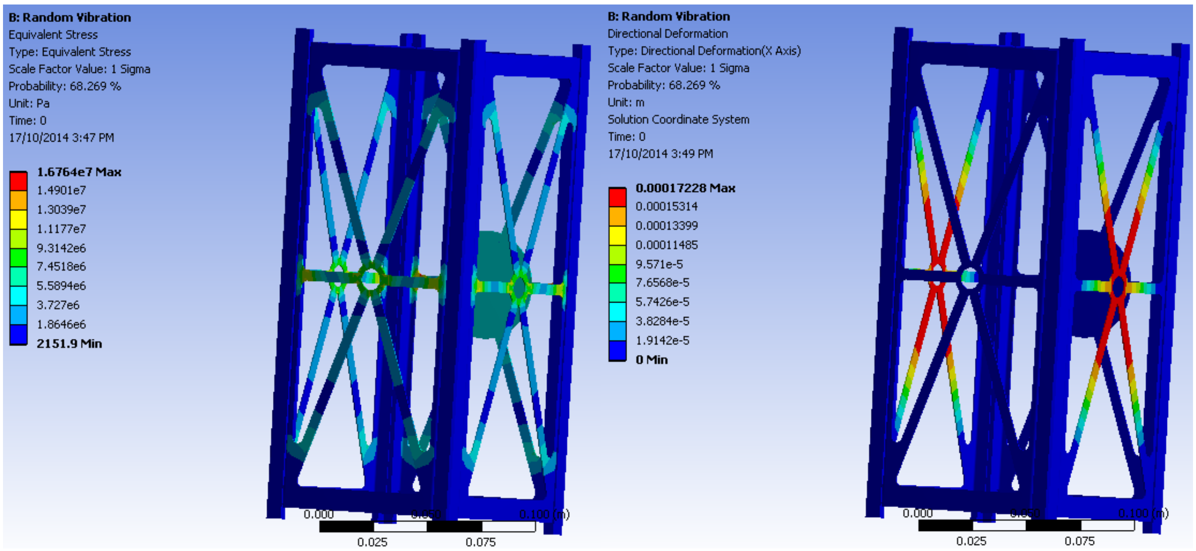

(a) **(b)**

Fig. 12. (a) von-Mises stress; (b) Max/Min deformation

The internal and external layout of I-INSPIRE II are shown in Fig. 13, the internal layout design will adopt PCB stack-up structure. Detailed layout and assembly procedures will be described in Document 3 “Assembly, Integration and Test Plan”

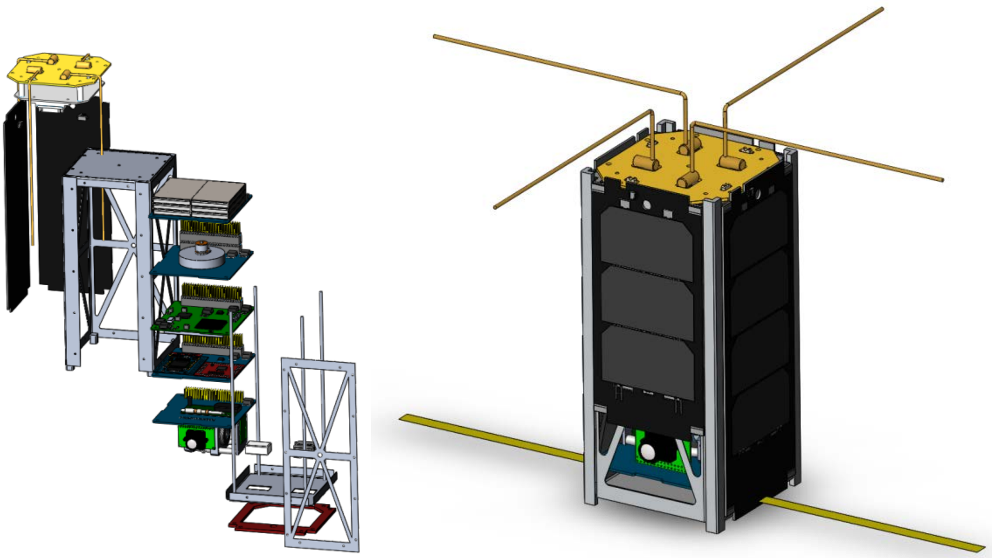

Fig.13 Layout of I-INSPIRE II

A detailed finite element analysis has also been conducted in with the satellite, including the major subsystems. The model we used for the detailed FEA analysis. The model includes the structure, solar panels, the OBC board, the communication board, the ADCS board, the EPS board, the reaction wheel, and the payloads board. Fig. 14 shows the simulation results of the quasi-static analysis. Fig. 15 shows the simulation results of the random vibration analysis. Fig. 16 shows the simulation results of the modal analysis.

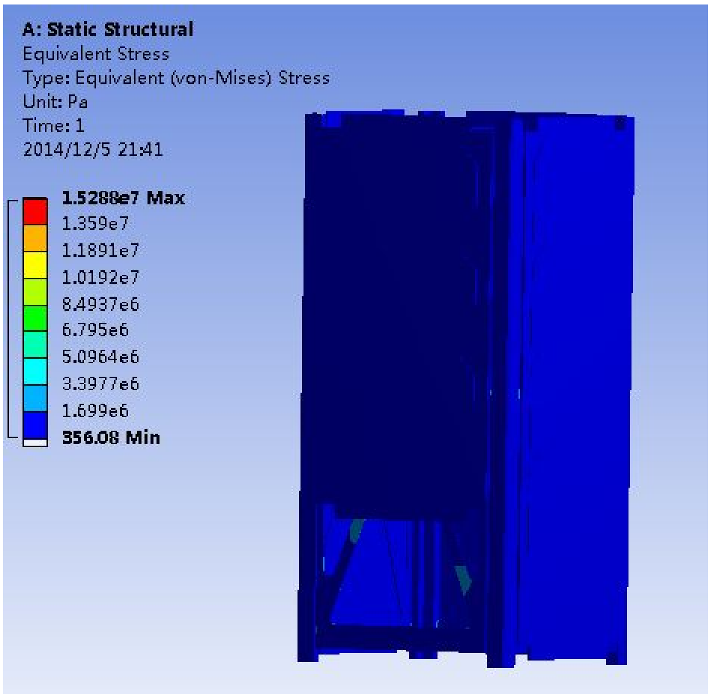

Fig. 14. Quasi-static ananlysis

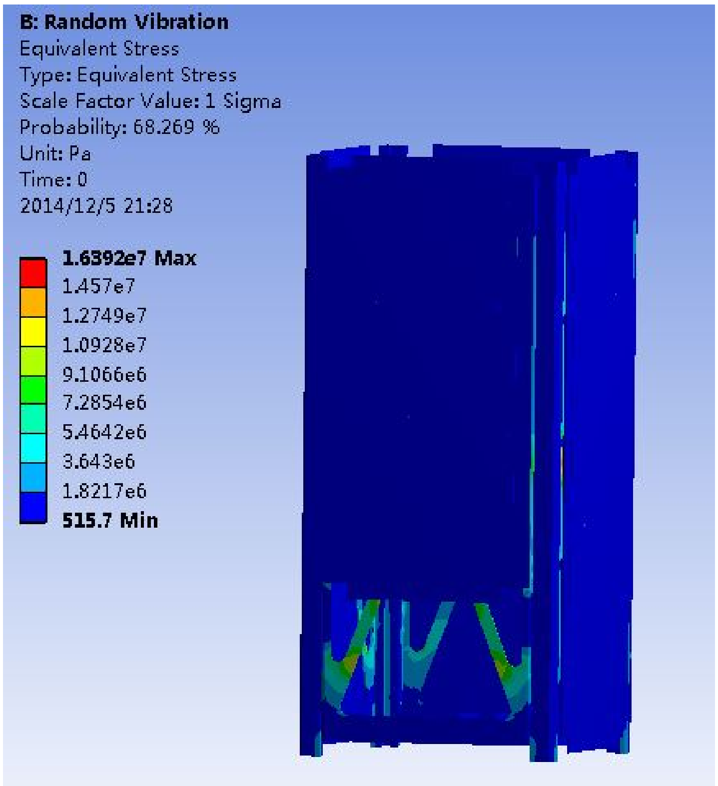

Fig. 15 Random vibration analysis

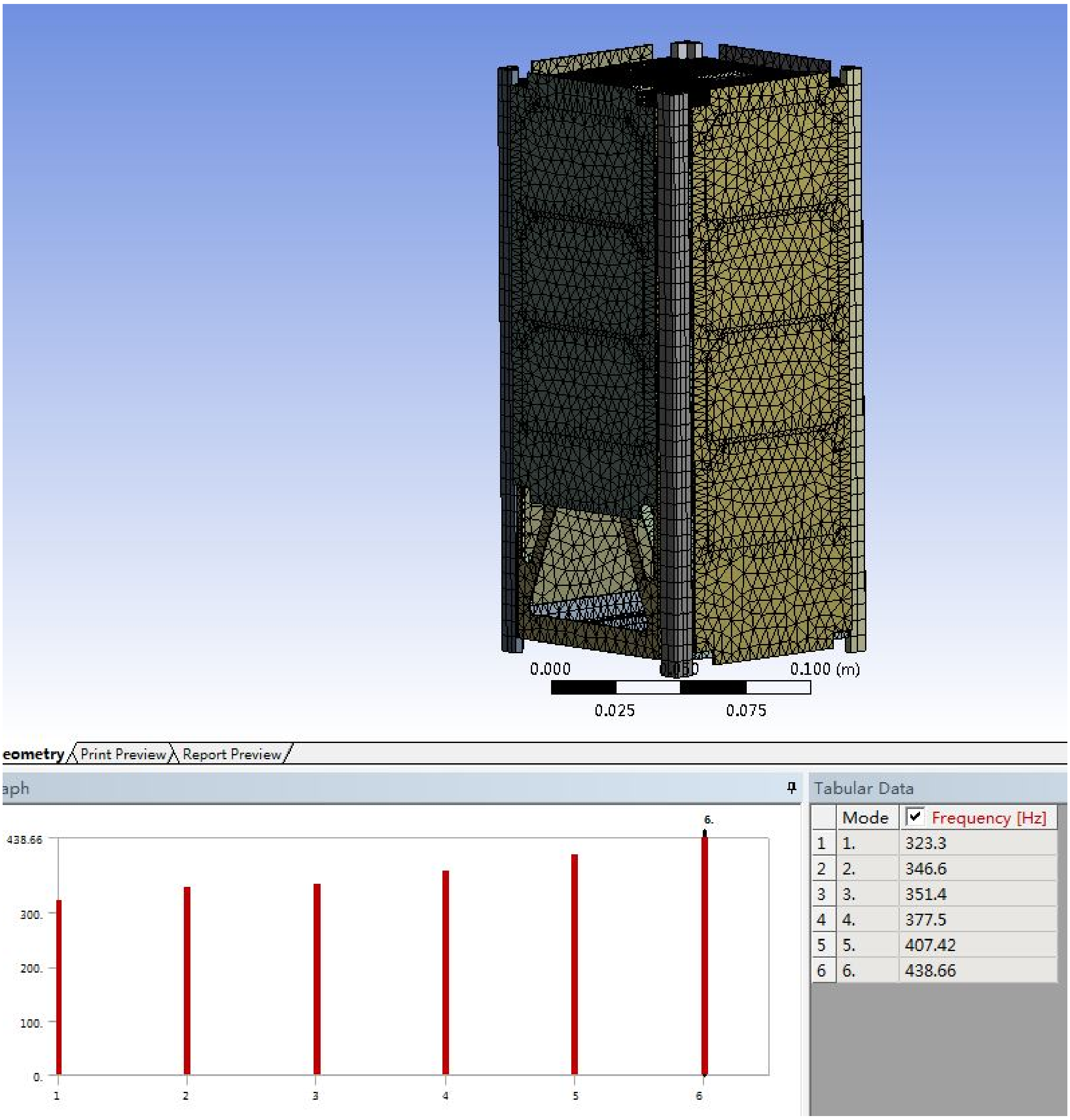

Fig. 16. Modal analysis

According to the simulation results, the satellite safety margin is 15.8, which meets the QB50 requirement.

Mass budget

The total mass of the CubeSat must be less than 2kg as mentioned in QB50 design requirement, however, due to the possible variations in future design, the contingency was decided to be added for each component. The mass budget of the I-INSPIRE II is given in Table 4. It shows that after the consideration of contingencies, the mass of the CubeSat is 1954.28 g, and it is still under the 2kg design requirement.

Table 4. Mass budget

Component	Per Unit Mass (grams)			*AU03* Mass (grams)		
	Estimated Mass	Contingency	Total	Quantity	Contingency	Mass
Attitude Determination and Control Subsystem						
z-axis magnetorquer	*50*	*5*	*55*	*1*	*5*	*55*
reaction wheel	*80*	*20*	*100*	*1*	*20*	*100*
IMU	*2*	*0.2*	*2.2*	*1*	*0.2*	*2.2*
Control driver circuit	*60*	*15*	*75*	*1*	*15*	*75*
Sun Sensor	*5*	*0.5*	*5.5*	*6*	*3*	*33*
Electrical Power Subsystem						
battery	*27.3*	*2.73*	*30.03*	*6*	*16.38*	*180.18*
2U Solar Panel W/MTQ	*82*	*8.2*	*90.2*	*2*	*16.4*	*180.4*
2U Solar Panel	*69*	*6.9*	*75.9*	*1*	*6.9*	*75.9*
1.5U Solar Panel	*48*	*4.8*	*52.8*	*1*	*4.8*	*52.8*
EPS board	*80*	*8*	*88*	*1*	*8*	*88*
On-board Computer and On-board Data Handling Subsystem						
MSP430H5438	*25*	*2.5*	*27.5*	*1*	*2.5*	*27.5*
Xilinx Spartan 6 LX150	*30*	*3*	*33*	*1*	*3*	*33*
Communication Subsystem						
GAMALink	*100*	*0*	*100*	*1*	*0*	*100*
ISIS transceiver	*85*	*93.5*	*178.5*	*1*	*93.5*	*178.5*
Structure						
MLI blanket	*10*	*2.5*	*12.5*	*1*	*2.5*	*12.5*
Structure	*200*	*50*	*250*	*1*	*50*	*250*
Payload						
mNLP	*225*	*22.5*	*247.5*	*1*	*22.5*	*247.5*
NanoSpec	*200*	*20*	*220*	*1*	*20*	*220*
Camera	*12*	*1.2*	*13.2*	*1*	*1.2*	*13.2*
Radiation Counter	*16*	*1.6*	*17.6*	*1*	*1.6*	*17.6*
Subtotal						*1854.28*
Integration						*100*
Total						*1954.28*
Target						*2000*
Margin						*45.72*

The centre of gravity is also defined in QB50 design requirement, it states that the centre of gravity shall be located within a sphere of 20 mm diameter. It can be concluded from Table 5 that this layout provides an acceptable centre of gravity. The moment of inertia is given by Table 6.

Table 5. Centre of Gravity of I-INSPIRE II (mm)

From Origin	From Geometric Centre
X=49.23	0.77 (Towards X-)

Y=50.36	0.36 (Towards Y+)
Z=109.67	2.83 (Towards Z-)

Table 6 Centre of Gravity of I-INSPIRE II ($\mathrm{g/mm^2}$)

Lxx = 1873452	Lxy = -376	Lxz = 5973
Lyx = -376	Lyy = 1876439	Lyz = 268
Lzx = 5973	Lzy = 268	Lzz = 653375

4. Attitude Determination and Control Subsystem

The attitude control and determination subsystem must firstly be able to detumble the satellite, and then be able to determine and control the attitude of the satellite. Given the nature of our mission, accurate satellite pointing is not overly important, however, the acceleration and rotation of the satellite must be precisely determined in order to obtain data on the thruster. It was thus determined that the following components would be required:

- 3 magnetorquers
- 1 reaction wheel
- 5 sun sensors
- 3 axis gyro
- 3 axis accelerometer
- 3 axis magnetometer
- 1 earth sensor

The magnetorquers used for the CubeSat are from Clyde-Space. One magnetorquer is integrated with the front solar panel and one integrated with the side solar panel. The other one is the standalone Z-axis magnetorquer. The magnetorques must have a large enough dipole moment to both quickly detumble and position the satellite. It was decided that the satellite should be detumbled within 2 hours of deployment, and should be able to perform a 90^{o} manoeuvre in 120 seconds. The time taken to perform these operations, according to the Satellite Service Ltd (http://mstl.atl.calpoly.edu/~bklofas/Presentations/SummerWorkshop2010/Barrington-Brown-magnetorquer.pdf), is shown below as a function of dipole moment (Fig. 17).

Given the design parameters above, a magnetorquer with a dipole moment of at least 0.1Am^2 is required. And the Clyde-Space's magnetorquers can meet the requirement with the minimum dipole moment being 0.14 Am^2. The copper coil wires require a 5V power source to operate, and each coil will typically use up to 200mW. Each coil is operated through an H-bridge to allow the magnetorquers to produce bi-directional moments.

To increase the pointing accuracy, in i-INSPIRE II we also include an in-house built reaction wheel at the Z-axis. The reaction wheel uses a flat DC motor from Maxon Motor (EC-14). The reaction wheel was built and tested on a 6 degree-of-freedom air-bearing table as shown in Fig. 18. With hardware-in-loop test, the attitude control can obtain an accuracy of less than 1^{o}, which considers the IMU, controller and reaction wheel.

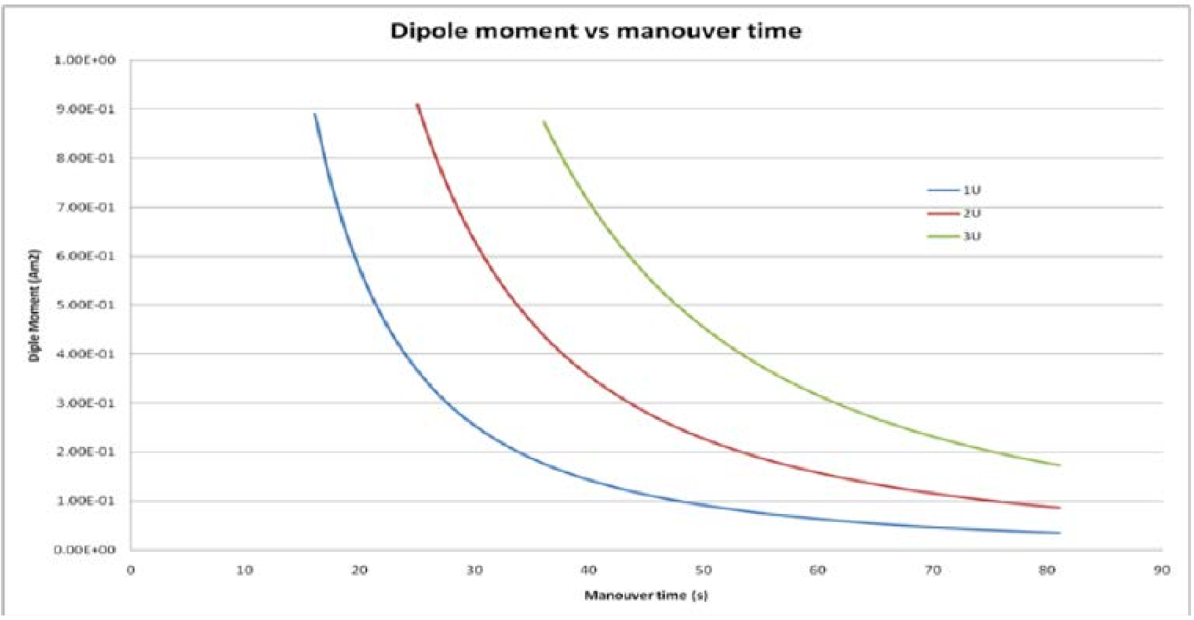

Fig. 17 (a). Dipole moment v.s. manoeuvre time

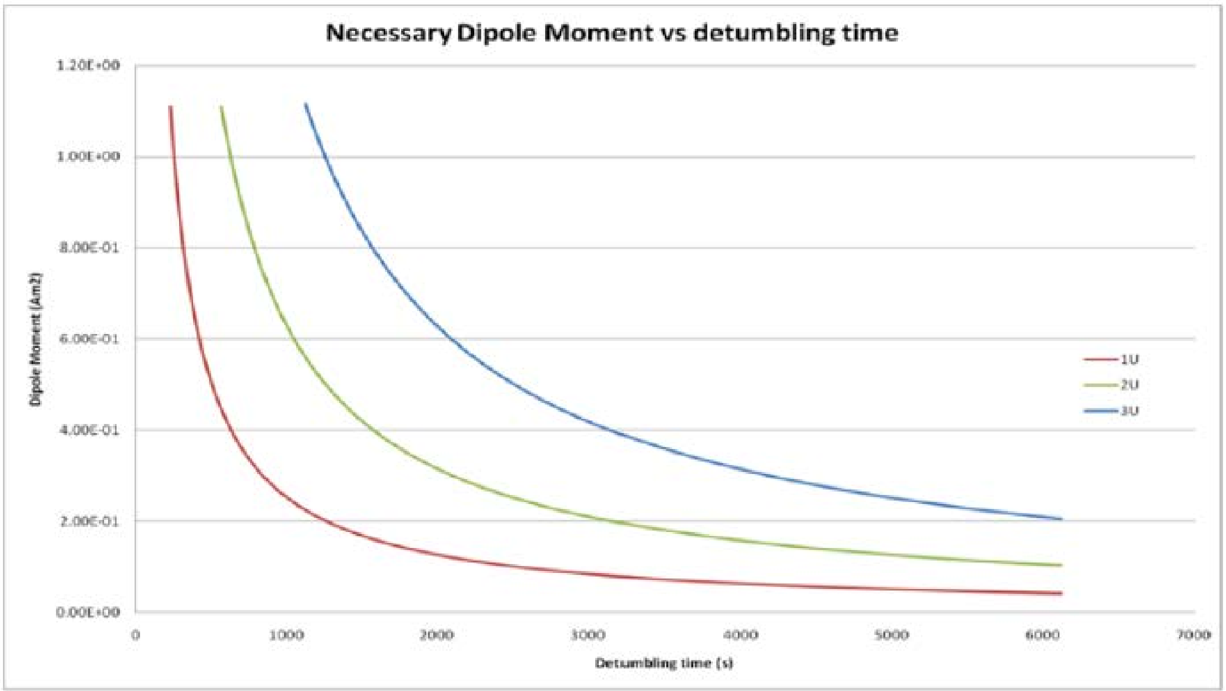

Fig. 17 (b). Dipole moment v.s. detumbling time

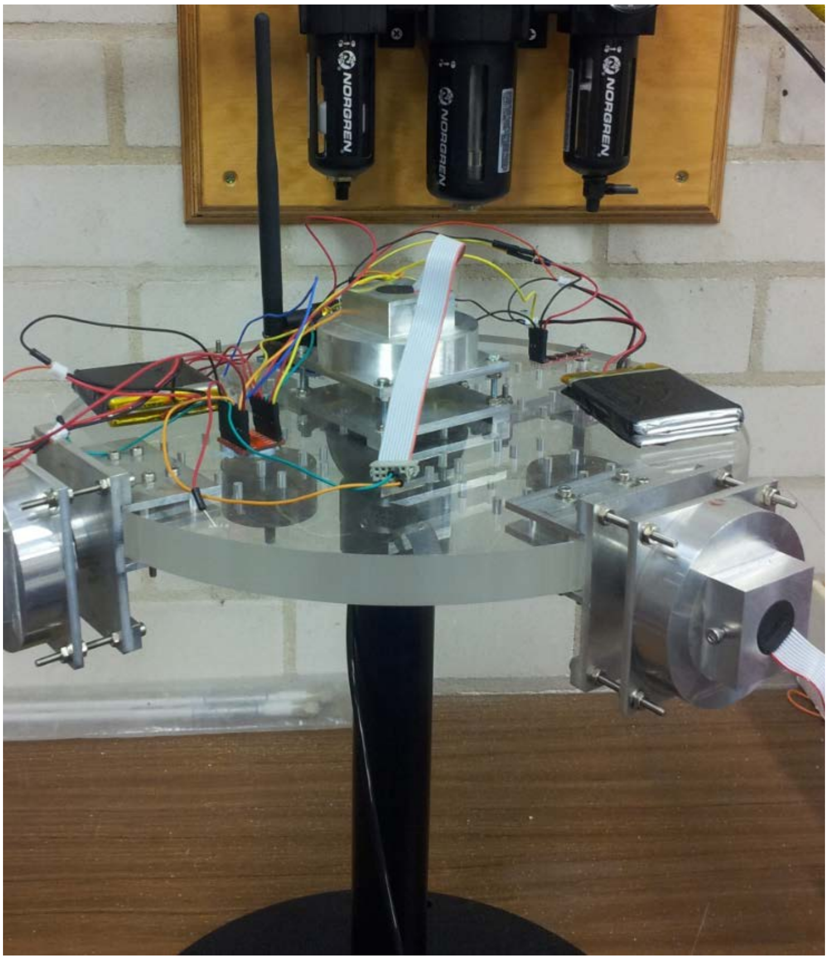

Fig.18 In-house built reaction wheels testing with airbearing table

Rather than using 3 separate boards for each of the accelerometer, gyro, and magnetometer, a single board with all of these components is used to save space and make for simplicity. The board chosen for the CubeSat is the Sparkfun SEN-10724 9 Degrees of Freedom Sensor Stick. The board has small form factor of just 34.8mm x 10.7mm x 2.4mm, making it ideal for nanosatellite applications. The board contains an ADXL345 accelerometer, a HMC5883L magnetometer, an ITG-3200 gyro and 6 home-made sun sensors. The Sensor Stick requires a 3.3V connection to the power supply unit. The power drawn by Sensor Stick is negligible. Like many other components in the satellite, the Sensor Stick has a simple I2C to communicate with the main processor of the satellite. It will provide data to the OBDH system of the satellite. At the same time, the OBDH will use the payload camera as the earth sensor and the solar panels to determine the rough pointing direction of the satellite. And a PID controller will use this information to control the magnetorquers.

The inertial matrix of the i-INSPIRE II satellite is shown in Table 6. It is treated as being symmetric about all three axes when we design the control algorithm. However, the mass centre is not strictly at the geo-centre of the satellite, we consider the torque generated due to the asymmetry as a white noise. And this noise will be added to the control loop together with other disturbance torques.

We consider a 2U CubeSat (20cm*10cm*10cm) using the reaction wheel for Z-axis attitude control. The maximum torque generated by the reaction wheel is $1.72 \times 10^{-5}\mathrm{Nm}$. In the following simulation, we take $1 \times 10^{-5}\mathrm{Nm}$ as the hard constraint as the control torque.

Having multiple means of determining the CubeSat's attitude is essential for accurate and reliable measurements, as well as to provide some redundancy in case of sensor failure. The satellite's ADCS subsystem employs both an inertial measurement unit (IMU) and a sun sensor to determine the CubeSat's yaw, pitch and roll. Measurements from either of these sensors are fused by way of a complementary filter which takes into account the reliability of the measurements taken from each sensor.

Data from the gyroscope and the accelerometer is fused via an algorithm running on the main OBC in order to determine yaw, pitch and roll. The on-board algorithm utilises the direct cosine matrix (DCM) to fuse data from each sensor. In this algorithm, normally the accelerometer and the IMU are initially used to define the coordinate axes with respect to which yaw, pitch and roll are calculated, with the IMU providing the direction of the gravity vector ('down') and the magnetometer giving the direction of the North vector. As these two vectors are orthogonal, they allow for determination of the 3rd vector, thus fully defining a set of coordinate axes.

In this mission, sun sensors are used as a method of determining orientation of the CubeSat. Sun sensors make use of the sun's high luminosity relative to other astronomical objects and its relatively small diameter seen from an orbiting object near the Earth's surface. The sun sensor system utilises differences in Light Dependent Resistors' (LDR) angle and sensitivity to provide an approximate unit vector that determine the relative position of the sun from the CubeSat's body frame. The satellite uses the 'two face couple measurement' method of attitude determination tested in the development of the ADCS subsystem as shown in Fig. 19. n is the normal vector from each face and t is the tangential vector, s is the vector (to be determined) towards the Sun.

This configuration enables readings of angle α to be made at the same time the sun vector s can be projected on the n-t plane. However, the value of alpha only indicates pitch angle. In order to provide a complete unit vector measurement, another set of LDRs is required. The two orthogonal sets of LDRs generate relations which allow the intensity of sunlight at different incident angles to be determined, which is then converted to an angular displacement to the Sun.

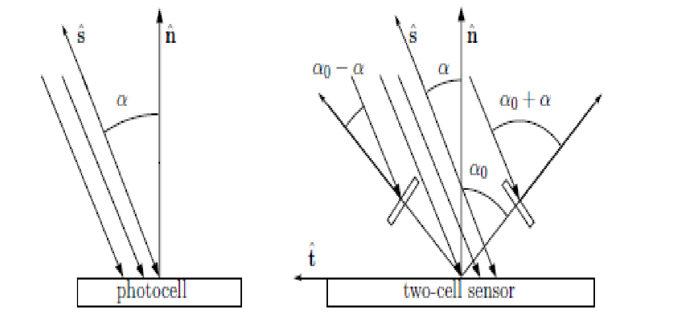

Figure 19. Sensor/Photocell Orientation.

This method is able to give a 10 degree precision in measurement, which is sufficient for our payload pointing requirements.

The actuation component of the ADCS consists of magnetorquers interfacing with the on board controller for control. The circuit required to generate required magnetorquer responses from input PWM signals at different duty cycles is shown in Figure 20.

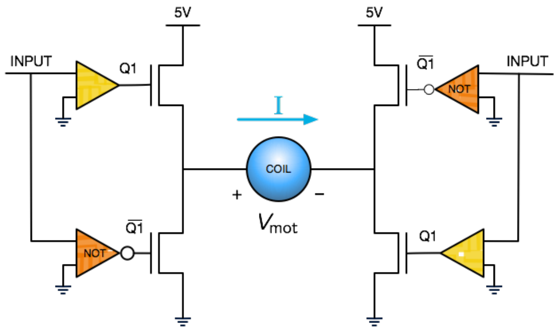

Fig. 20. The H-Bridge for driving magnetorquers

The physical disturbance forces expected in the CubeSat's operating environment are aerodynamic torque, and to a lesser extent gravity gradient and radiation pressure.

The maximum torque output of the magnetorquers is a function of the current through them, the geometry of the magnetorquers and the strength of magnetic field the CubeSat is in.

$T_m = 2.2 \times 10^{-6}\ N \cdot m$ was determined to be the maximum available torque. This is sufficient for the detumbling and recovery requirements prescribed by QB50 at 380 km. According to the mNLP requirement, it needs to operate at least 200 km. At 200 km, we calculated the maximum disturbance torque, including atmospheric drag, solar pressure and gravity gradient. It is about $T_d = 1.0 \times 10^{-6}\ N \cdot m$. In this case， the magnetorquer can generate higher torque than the disturbance torque; hence, the attitude control system can work at least at 200 km.

The PID control algorithm used to determine command values of yaw is outlined in Figure 21. The simulated controller was designed to minimize the steady state overshoot while maintaining fast transient response, under the constraints of the relatively weak actuation. The disturbance torques and noises due to the asymmetry are added to the actual control signal, and fed into the satellite dynamic model.

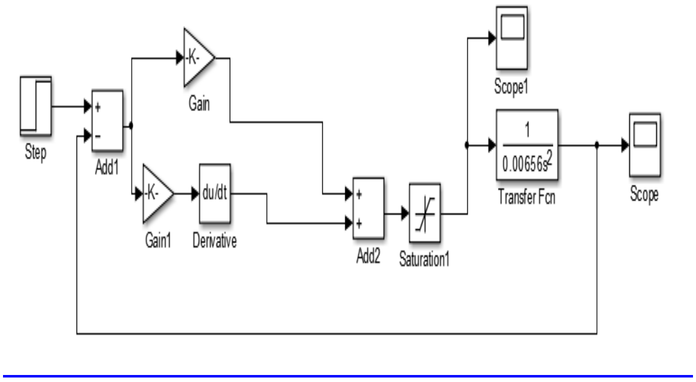

Fig. 21. Simulink model of the PID control algorithm

The satellite also equips an in-house built reaction wheel about z-axis. The maximum torque generated by the reaction wheel is $1.72 \times 10^{-5}\mathrm{Nm}$. In the following simulation, we take $1 \times 10^{-5}\mathrm{Nm}$ as the hard constraint as the control torque.

For active pointing, a simple PID control algorithm is developed. Fig. 22 shows the comparison between the Matlab simulation results (red) and the hardware-in-loop simulation (HILS) results (blue). The HILS includes the Matlab, which runs the satellite dynamic model, and the MSP430 controller, which runs the control algorithm.

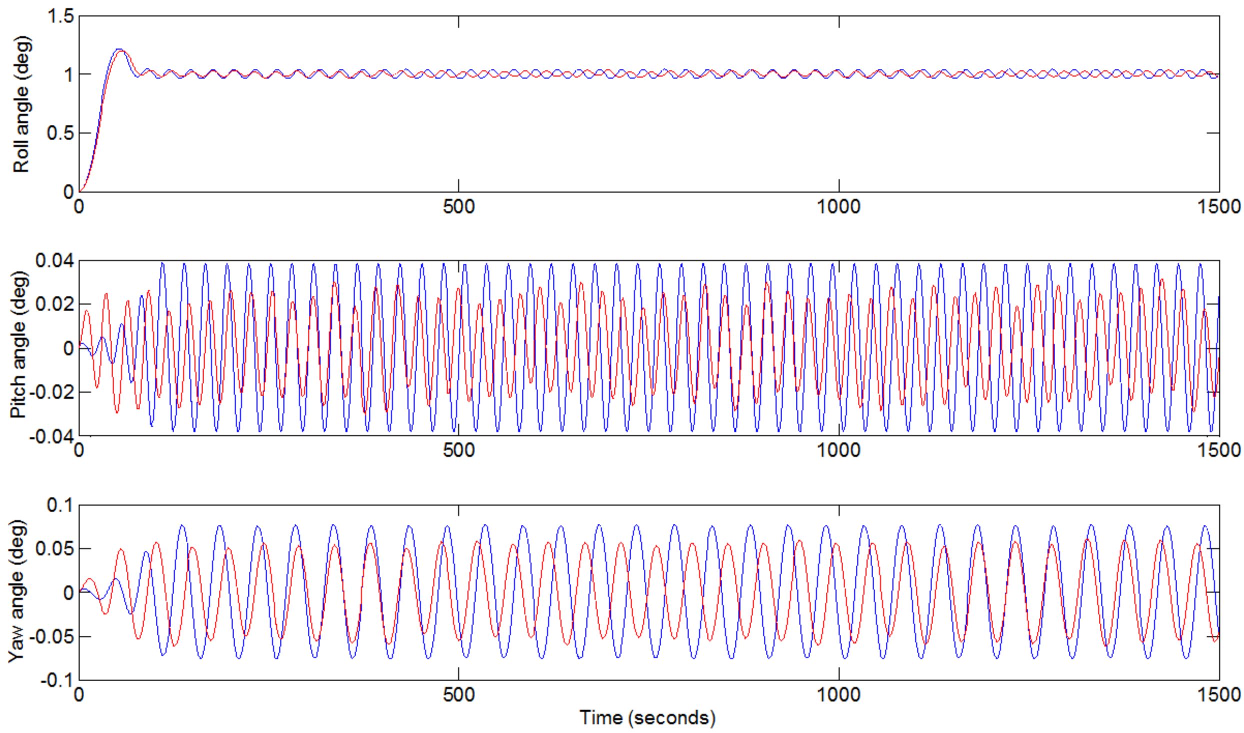

Fig. 22. Satellite Pointing

From the simulation results, we can find that the satellite's pointing accuracy is between -0.1° and 0.1° with the reaction wheel as the actuator and the gravity gradient, atmospheric drag, solar pressure and asymmetry noise as the main disturbance sources.

We have two attitude actuators: the magnetorquers and the reaction wheel. As the magnetorquers have already met mNLP's pointing requirement. Hence, for the satellite attitude control, we will use the magnetorquer 95% of each orbit. However, we will use the reaction wheel for fast response to the control torque. Especially, when the pointing error about z-axis is over 10 degrees, the reaction wheel will be used to bring back the satellite to the desired pointing direction quickly.

5. Electrical Power Subsystem

The EPS module includes the solar panels, batteries and the power management board. As the requirement of stabilization for the QB50 mission, in our design, we use four solar panels from Clyde-Space: one 2U front solar panel with magnetorquer at X+ and one 2U side solar panel with magnetorquers at Y+, one 2U front solar panel at X- and one 1.5U side solar panel at Y-. The specification of the power panels are:

- PCB thickness: 1.6mm
- With magnetorquers
- Mass : 98g
- Power: 5.2W @ 28^{o}C

The batteries selected for the CubeSat is the VARTA Li-Po LPP 454262 8TH. This battery was chosen for its high capacity in a compact size. Main specifications, supplied from the manufacturer, are listed in Table 7. The batteries will only charge between 0 ^{o}C and 40^{o}C and discharge between -20 ^{o}C and 60 ^{o}C. It is important that the batteries can discharge at low temperatures, especially during the Eclipse. The thermal analyses (Section 8) of the satellite we have indicate that it is sufficient using passive thermal control.

Table 7 Battery specification

Type	Lithium Polymer
Dimensions (l × w × h, in mm)	61 × 42 × 46
Weight (g)	27.3
Voltage (V)	2.85 to 4.2 (3.7 Average)
Capacity (mAh)	1590
Charging Voltage (V)	4.2
Charging Current (Min/Normal/Rapid) (mA)	318/765/1530
Charging Time (Normal/Rapid) (hrs)	3/2.5
Maximum Discharge Current (mA)	1530

The battery detailed in Table 7 above would need to be used during times of eclipse, which, when simulated was found to be approximately one-third of the time for the 90 minute orbital period. During this time, the battery is the sole source of power, and initial designs include 3 sets of 2 batteries. Each set would contain a pair of batteries in parallel, to bring the capacity up to

3.18 Ah. The multiple packs of battery allow for simultaneous charging of one set and discharging of another set.

This configuration was selected to allow high powered components to be active during the eclipse. During this time, if the battery is depleted, considering that the solar panels can only generate approximately 1A current, charging the battery would significantly reduce the current available to the components. With this multiple sets of batteries, one set could be charged at the same time as another set is being discharged as a power supply for the components, thus maintaining the current flow.

The QB50 power management board is used to regulate the power supply from both the solar panels and the six supplementary batteries (three sets of two). Power supply from the solar panels is divided into four lanes, with Schottky barrier rectifiers limiting the direction of current flow, and current sense amplifiers. This is then regulated by a Low Dropout-Voltage (LDO) regulator, with an output of 4.2V. The LDO regulator helps to negate the effects of fluctuating voltage and outputs a constant 4.2V. The circuit is then connected with the battery sets, and split into two pathways. The first incorporates a boost converter, converting the voltage to 5V; the second, a buck-boost converter, converting the voltage to 3.3V. The power is then distributed to through the standard PC/104 stack. An Analog-to-Digital (ADC) converter acts as the interface between the current sense amplifiers and the main processing unit.

The components of the power management board are listed in Table 8.

Table 8 Components list for the power management board

Name	Brand	Type
LTC 3872	Linear Technology	Boost Converter
LTC 3533f	Linear Technology	Buck-Boost Converter
CRS 06	Toshiba	Schottky Barrier Rectifier
MAX 1112	MAXIM	Analog-to-Digital Converter
MAX 9929	MAXIM	Current Sense Amplifier
TPS 758A01	Texas Instruments	LDO Regulator
LPP 454261 8TH	VARTA	Li-Po Battery
3520	TE Connectivity	Resistor
DR 124	Coiltronics	Inductor, shielded
2600	Murata Power Solutions	Inductor, shielded
FDC637AN	Fairchild Semiconductor	MOSFET

A simplified schematic of the power management subsystem is shown in Fig. 23. As it shows, a separate circuit from the battery to the converters allows for simultaneous charging and discharging of two different battery sets.

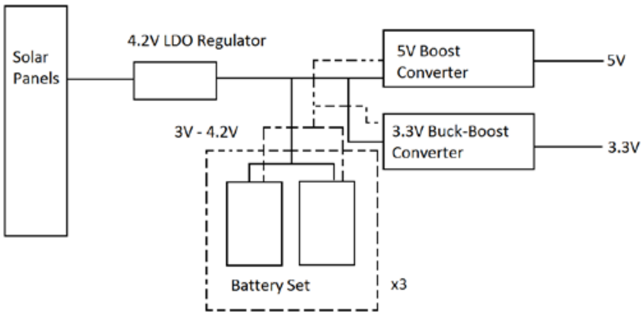

Fig. 23 The simplified schematic of the power management system

Using an ADC the battery voltage drop across the supply battery is measured, once the voltage drops to 3.2V, the supply battery is swapped to the previously charging battery using the MOSFET switch and now the discharged battery is charged. The switches are controlled by a digital signal from the OBC. Another major problem was continuously supplying power whilst the system is switching batteries. To avoid temporary loss of power during switching, a large switching capacitor of 2200uF was implemented to stop the power from ever being cut to the system. As a result, the system was able to deliver uninterrupted power to all of the subsystems. The complete circuit design is shown in Fig. 24.

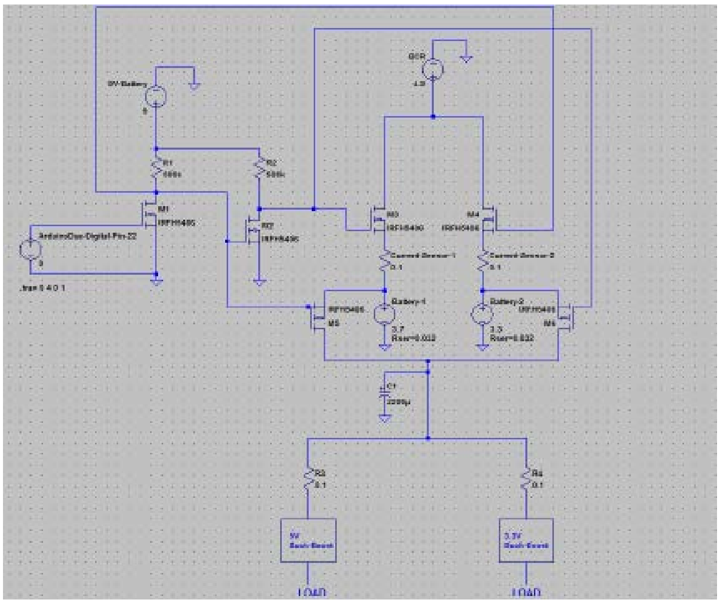

Fig. 24. EPS circuit design

With the capability of switching between batteries, we are able to ensure we have enough power to operate the satellite. In particular, in the worst case scenario if the satellite's Z panel is facing to the sun, the solar panel generates smallest amount of energy. In this case, the satellite will use the batteries to rotate the satellite to its normal pointing direction.

For the energy generated, it is important to calculate the effective area of the solar panels exposed to the Sun. Also according to ClydeSpace, the efficiency of the solar panel is 90%. Fig. 25 shows the effect sunlit area depending on the satellite's position. We can see that the effective area is between 1 and 2 solar panels for about 10 hours in each day; and the average power in this period is 1.414*5.2*0.9W. Also the effective area is between 0 and 1 solar panel for about 8 hours; and the average power in this period is 0.707*5.2*0.9W. The eclipse time is about 6 hours. In this case the total energy generated in one day will be 92.64 Whr.

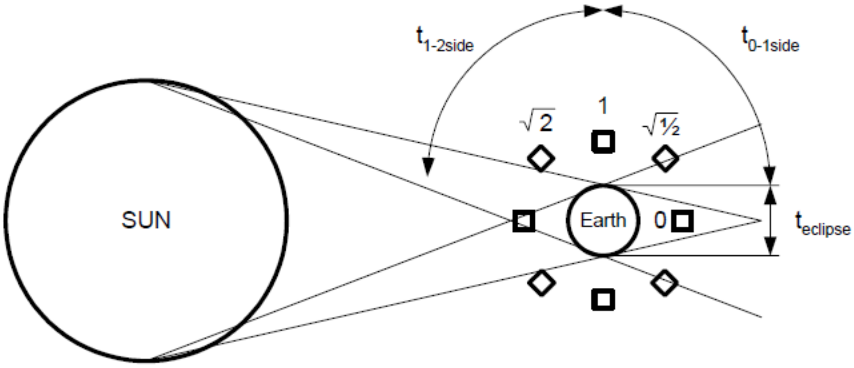

Fig.25. Effective sunlit area of the CubeSat.

The power budget is shown in Table 6, in which the duty cycle indicates how long each subsystem will run in each program loop. We assume the satellite is stabilised and working in the different modes. In this case, for each period the satellite can receive 3.86W in average. In some modes, the solar power is not enough to operate all the components. In this case, the battery will provide additional power. For detailed power budget under different modes, please see the CubeSat overview spread sheet. However, in this table we are concerned on the energy consumed and energy generated to ensure our satellite meet the power budget. According to this table, the incoming energy is considered enough for our planned mission

Table 9 Power budget

Load	Power consumption (W)	Duty Cycle (hrs/day)	Energy (Whr/day)
OBC (MSP430)	0.320	24	7.68
OBC (FPGA)	2.0	1	2
VHF Rx	0.35	24	8.4
UHF Tx	2.0	2	4
S-band Tx	1.5	2	3
S-band Rx	0.5	2	1
Reaction wheel	3.0	1	3

Magnetorquers	0.25	24	6
Power board	0.1	24	2.4
IMU	0.25	24	6
Science Unit Set	0.5 (@3.3V)	24	12
Camera/Earth sensor	0.100	24	2.4
GPS	1	6	6
NanoSpec	0.270	2	0.54
Radiation Counter	0.110	2	0.22
Total Energy consumed			64.64
Energy Generated			92.64
Energy available			28

However, in eclipse, the satellite won't receive any power from the Sun. In this case, it is necessary to investigate whether the battery can provide enough power to operate the satellite and the science unit. During eclipse, the active subsystems will be the OBC, VHF RX, UHF TX, magnetorquers, EPS board, IMU, Science Unit, GPS. According to the table above, the maximum power requirement is 4.37 W. And a battery set with two batteries can provide maximum power of 1.53*3.7*2=11.32 W, which is far enough. For the worst case scenario, the satellite's action will rotate the satellite to its normal pointing direction. In this case, the active subsystems will be the OBC, VHF RX, VHF TX, magnetorquers, reaction wheel, EPS board, and IMU. In this case, the maximum power requirement is 6.27 W. Again the battery set can provide enough power for this scenario. If we consider the total energy consumption during 6 hours' eclipse, with the duty cycle, the total energy consumption will be 10.72 WHr to operate the mNLP. The total energy available from one set of batteries is 1.59 Ah * 3.7 V *2 = 11.76 WHr, which is again sufficient for the mission. Table 9 also shows that the solar panel will generate enough power in each orbit. The solar power can be used to recharge the batteries.

6. On-Board Computer and On-Board Data Handling Subsystem

The I-INSPIRE II OBDH will consist of two parts: the on-board computer (OBC) and the on-board computer coprocessor (OBCC). External interfaces for programming and debugging on the ground will be one JTAG port and one USB serial port each computer. In this case, for the two hatches in the satellite structure, we will have two JTAG ports (6 male pins each) and two USB ports (4 male pins each) attached to allow program and debug the on-board computers.

OBC

The main OBC will be a low power COTS microcontroller from TI's MSP430 series, specifically the MSP430F5438. We will use a COTS board from Olimex, as shown in Fig. 26. The OBC will be responsible for the general operation of the satellite including managing telemetry, payload data collection, parsing ground station commands and running attitude determination algorithms. Housekeeping software will be adapted from the original I-INSPIRE I and expanded to be a fully interrupt driven system with increased data-handling capabilities.

Fig. 26. MSP430 Head Board for OBC

Two 256 MB SPI Flash memory will be attached to the OBC for data storage; this is more than sufficient storage for the minimum science data requirements even in the event of ground link unavailability but will also be used as intermediate storage for any online data processing. Inter-chip communication between the OBC and OBCC will also be facilitated by this SPI bus (OBC master, OBCC slave). The OBC will also be responsible for turning the entire OBCC on and off. A power FET acting as a switch will be placed in the power rails feeding the OBCC which may be controlled via digital I/O from the OBC; the OBCC will only be powered at all in certain operational modes.

The OBC will be connected to other subsystems physically using the PC/104 stack connectors and logically using two I2C interfaces. One I2C interface will be for telemetry only, connecting the various temperature sensors and current monitor ADCs etc., while the other will be used to command the other subsystems and/or send data to or collect data from them; this includes the science unit but not the other University of Sydney payloads (camera, Nanospec, radiation counter) which will be connected via UARTs.

The OBC will accept ground station commands as ASCII characters and transmit an acknowledgement when a command is received. The operational modes for the spacecraft can be seen in Table 10. The MSP430 also includes a watchdog timer which will be used to prevent stalls.

Table 10 Spacecraft operational modes

Spacecraft Mode	Description
Safe Mode	This mode is intended to keep the satellite alive. Only OBC (MSP430), EPS and receiver are on. Transmitter on only for intermittent beacons. Has uncontrolled attitude.
Recovery mode	This mode is used to de-tumble the spacecraft after ejection from the deployment dispenser as well as to recover it from any spin-ups. In addition to safe mode subsystems, the ADCS is active. Transmitter on only for intermittent beacons. Other subsystems can be turned on via ground uplink
Normal mode	All non-payload subsystems active. Transmission of full telemetry data. Payload systems can be turned on via ground uplink.
Science mode (I)	In addition to Normal mode systems, the scientific payload systems are active and collecting data.
Transmission mode	As Normal mode but telemetry and full payload data will be sent to the ground station.
Optional mode:	
Dual processor mode	In addition to Normal mode systems, the OBC coprocessor (OBCC) (Spartan-6) is active, mirroring the function of the main OBC.
Science mode (II)	As Science (I) mode but the OBCC is active, managing data collection as well. Any online processing is split between MSP430 and FPGA processors.

The state machine for these operational modes can be seen in Fig. 27. Transitions for the spacecraft modes will mostly be by command from the ground station, however there will be provision for the spacecraft to automatically transition to the data collection modes and collect the minimum amount of required data per day if ground station contact is unable to be established for that day.

Transmission of the payload data will be initiated by the ground station but will utilise a Direct Memory Access (DMA) channel for actual transmission leaving the processor free for other tasks once the transmission is underway. A number of the error mode transitions also exist; these are omitted from Fig. 27 for clarity but are outlined below in Table 11.

Table 11 Transition to safe mode

Error	Description	Transition
Low battery	Battery charge levels < 15 %	From Any mode to Safe mode
Spin-up	Detection of anomalous spin rates after de-tumbling (> 10° pointing error, > 1 °/s rate))	From Any mode (not Recovery mode) to Safe mode
Software stall	Stalls detected by the watchdog timer	From Any mode (soft-reset) to Safe mode

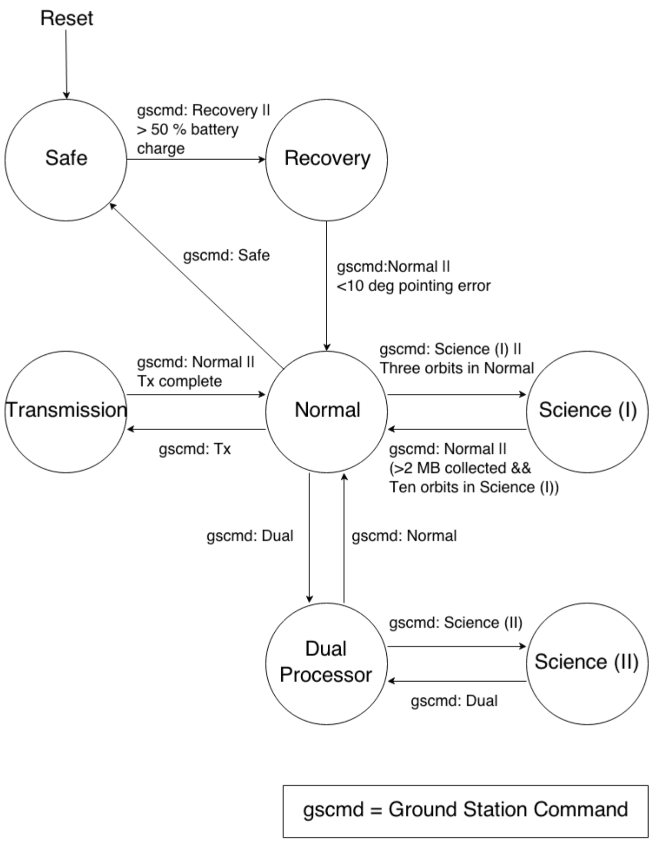

Fig. 27 State machine for satellite operation

To operate the scientific unit, in our case the mNLP, the OBC will follow the script format to read in each command packet, decode it and perform the action required by sending the command packet to the MNLP_SU for execution. Upon the telecommand, the satellite is also able to download the science data while operating the mNLP.

OBCC

The additional OBCC module as shown in Fig. 28 will be a COTS development board from Enterpoint, the XC6SLX150 X1 Coprocessor Module, based on a Xilinx Spartan-6 FPGA. The OBCC will be used to test a number of experimental approaches to FPGA-based computing for aerospace applications. This includes direct-to hardware implementations of complex algorithms to complement the OBC and soft-core processors mirroring the function of the OBC. Whichever approach is being tested, the OBCC remains entirely optional and no critical functions for the satellite will be run on it. When in the relevant operational modes, the OBC will pipe incoming raw data over the SPI link to the OBCC.

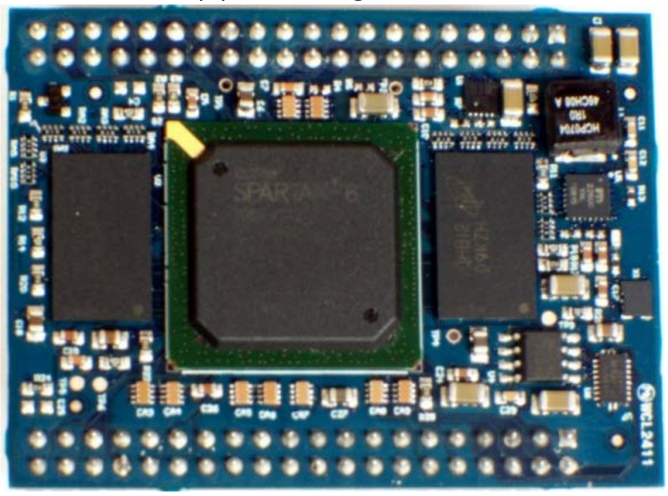

Fig. 28 The OBCC with Xilinx Spartan 6 FPGA

7. Communication Subsystem

GAMALINK

For the communication subsystem, we will collaborate with the GAMANET team and use the GAMALINK. The main operating mode in GAMALINK is advanced mode. This is where the full capability of GAMANET is demonstrated, ISLs are established and the CubeSats throughput is greatly improved. This mode uses S-Band and data rates up to 1 Mbit/s. However, GAMALINK will have an optional operation capability, called compatibility mode. In this mode, the platform operates in the UHF/VHF amateur radio bands, using direct links with Ground and packets are exchanged using the typical AX.25 protocol using lower data rates. The main objective of this mode is to give teams an optional operating mode in a common radio amateur format, greatly improving the redundancy in GAMALINK and their satellite tracking capability from Ground. Switching between communicating modes can be done via an OBC command and it will be up to each CubeSat Team to determine their communication approach. For instance, compatibility mode can be used briefly every orbit, just to send out housekeeping information. It is important to note that the UHF/VHF antennas are not provided with GAMALINK. Table 12 lists the specifications of the GAMALink module.

Table 12. GAMALink Specifications

Frequency: Downlink Uplink	S-band (2.40-2.45 GHz)	UHF (430-440 MHz) VHF (144-148 MHz)
Bandwidth: Downlink Uplink	40 MHz	20 kHz 10 kHz
Data Rate: Downlink Uplink	up to 1 Mbit/s	9600 bps 1200 bps
Protocol	GAMANET	AX.25
Positioning precision	5 m (GPS)	
GPS update rate	5 Hz	
GPS message format	SiRF-like binary (NMEA available on request)	
PCB size	95.9 x 90.2 x 11 (mm)	
Total PCB mass	< 100 g	
Antennas: 3-axis stabilised Spinning	4 (3 S-band + 1 GPS) 10 (6 S-band + 4 GPS)	To be defined by Teams
Antenna size: S-Band GPS UHF/VHF	approx. 15 x 15 (mm) approx. 20 x 20 (mm) To be defined by Teams	
Data Interface	UART, others available on request.	
Storage Capacity	2 x 2 GB	
Supply Voltage	3.3V (5V also available)	
Average Power Consumption Transmitting	< 1.0 - 1.5 W (depending on configuration) < 200 - 500	

Receiving	mW (depending on configuration)

GAMALINK supports UART, SPI and I2C protocols. For i-INSPIRE II, we will use I2C protocol between the MSP430 microcontroller and the GAMALINK. The GPS on-board the GAMALink will be used to determine the position of the satellite.

ISIS transceiver

As the GAMALink is allowed only for secondary communication, the main communications subsystem will be based on the ISIS UHF downlink / VHF uplink full duplexer transceiver. The specification is listed in table 13.

Table 13. ISIS transceiver specifications

Specifications	Product properties
UHF transmitter	
Frequency range: 400-450MHz (Synthesized)	Mass: ~ 85g
Transmit power: Typical 500mW.	Dimensions: 96 x 90 x 15 [mm]
Modulation: Raised-Cosine Binary Phase Shift Keying (BPSK)	Power: <2.0W (transmitter on), <0.35W (receiver only)
Data rate selectable: 1200, 2400, 4800, 9600 bit/s. Higher values on request	Interfaces:
Protocol: AX.25 (Other protocols available upon request)	
	104 pin CubeSat Kit stackthrough connector carrying:
VHF Receiver	5-18V DC power supply
Frequency range: 130-170MHz (Synthesized)	I2C bus interface
Modulation: Audio Frequency Shift Keying, 1200Hz/2200Hz (Bell202)	Raw FSK demodulator output
Data rate: 1200 bit/s.	Direct modulator input
-100dBm Sensitivity for BER 10E-5	RF input: MMCX 50 ohm
On-board AX.25 command decoding	RF output: MMCX 50 ohm

For QB50, it is required that the satellite needs transmit beacon signals at least every 30 seconds. Each beacon signal is 100 bytes. We tested the time required for transmitting beacon signals, including encoding, modulation and transmission. It takes less than 1 second to transmit one beacon signal. In this case, in most modes, we put 25% as the duty cycle for operating the transmitter. In the science mode, we won't operate the mNLP continuously. It will be turned on for about 30 seconds to get the science data; then it will be turned off. In this case, there will be no transmission during the science mode.

Antenna

The i-INSPIRE II satellite will use three antennas (as shown in Fig. 29), one for VHF, one for UHF and one for S-band. The VHF and UHF antennas are used by both GAMALink and ISIS transceivers. And the S-band antenna is used by GAMALink for inter-satellite communications. All the antennas will be flat turnstile antennas (crossed dipoles). The antennas are connected to the ISIS communication board using SMA connectors. The fundamental principle is to guarantee the 50Ohm impedance on transmission line and VSWR (Voltage Standing Wave Ratio) less than 1.5. In this case, we can maximize the delivered transmitting power.

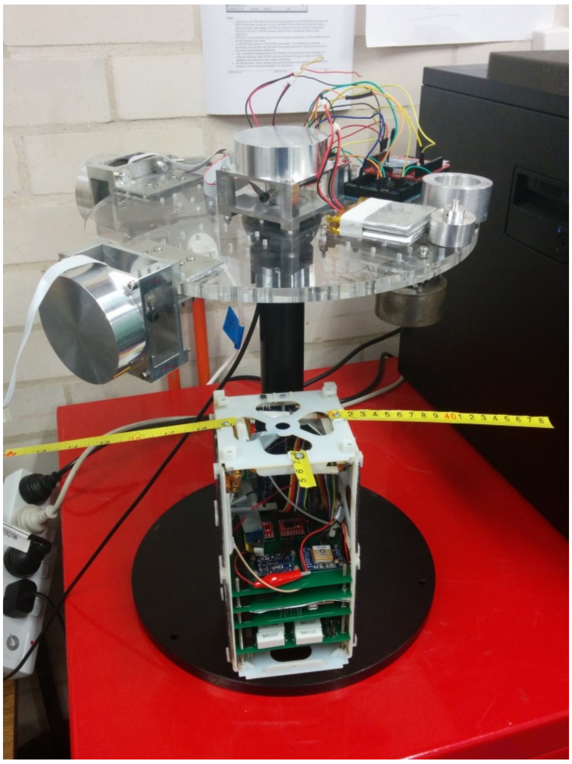

Fig. 29. Satellite antennas

In order to circumvent unpredictable polarization loss due to Faraday rotation in the atmosphere it has been concluded that the ground station must use circular polarization. In order to minimize the polarization loss it is also preferable with circular polarization on the spacecraft, which is one reason to use turnstile antennas.

Moreover, as the satellite will have a varying elevation angle as it passes the sky, the off-nadir angle will also change, and as a consequence, the antennas should be designed, not to be directive, but to optimize the link margin for as many elevation angles as possible. The turnstile antennas outperform several other commonly used antennas for CubeSats in this respect.

The antennas will be made of measuring tape wrapped around the satellite and tightened with nylon lines which will be burnt off by NiChrome-wire for deployment such that the measuring tape will restore to its original shape and form the elements of the turnstile antennas. This will be done sequentially to prevent jamming of the antennas.

Ground station

The ground station is of primary importance for mission success in the QB50 communication link. Its main purpose is to track and receive data from CubeSats for data analysis. Since all communication with CubeSats is done wirelessly, the ground station serves as the access point on Earth. The main functions of the Ground Station are:

1. Receive, process and interpret the QB50 data sent by the Space Segment;
2. Make the received data available to the other QB50 Ground Stations;
3. Send uplink commands to the Space Segment.

The ground station will include an ICOM model IC-9100 ham radio, a software defined radio for PSK and other modulations, power source, PC computers. And Antenna rotor provides 450^{o} azimuth and 180^{o} elevation control. The actuator can be controlled manually or an auto-tracking algorithm can be implemented by an appropriate software package to utilize the received satellite signal to steer the antennas.

The primary ground station to be used to communicate with the QB50 will be located at University of Sydney, Sydney Camperdown Campus. Multiple ground stations could be used if one ground station proves to be inadequate to downlink all science data.

The ground station of USYD in Fig. 30 shows the connections between the various components. As can be seen the UHF, VHF and S-band antennas are mounted on the same boom, through the rotor. This allows the auto tracking function to be controlled by a single motor. Auto tracking is enabled by the rotor-PC interface. The antennas are connected to the transceiver by coaxial cables, which are connected to the PC for further antenna operations.

Antenna frequency bands for i-INSPIRE II

a) S-band: It is a patch antenna for 2.4 GHz intended for use with a parabolic reflector 60 cm dish. It is designed to be attached to a dish via three support legs as illustrated Figure. This antenna dish has an f/d ratio of approximately 0.35, and a measured gain of 21 dbic.
b) UHF: The cross-Yagi UHF antenna can cover UHF frequency bands ranging from 430 to 438 MHz. Constructed entirely from aluminum, 42 elements can get 18.9 dBic gain. Return loss is optimized for better than -20 dB, less than 1.5:1 VSWR across the full band.
c) VHF: The cross-Yagi VHF antenna can cover VHF frequency bands ranging from 144 to 148 MHz. It operates with 14.39 dBic (or 12.25dBd) gain and 1.4:1 VSWR.

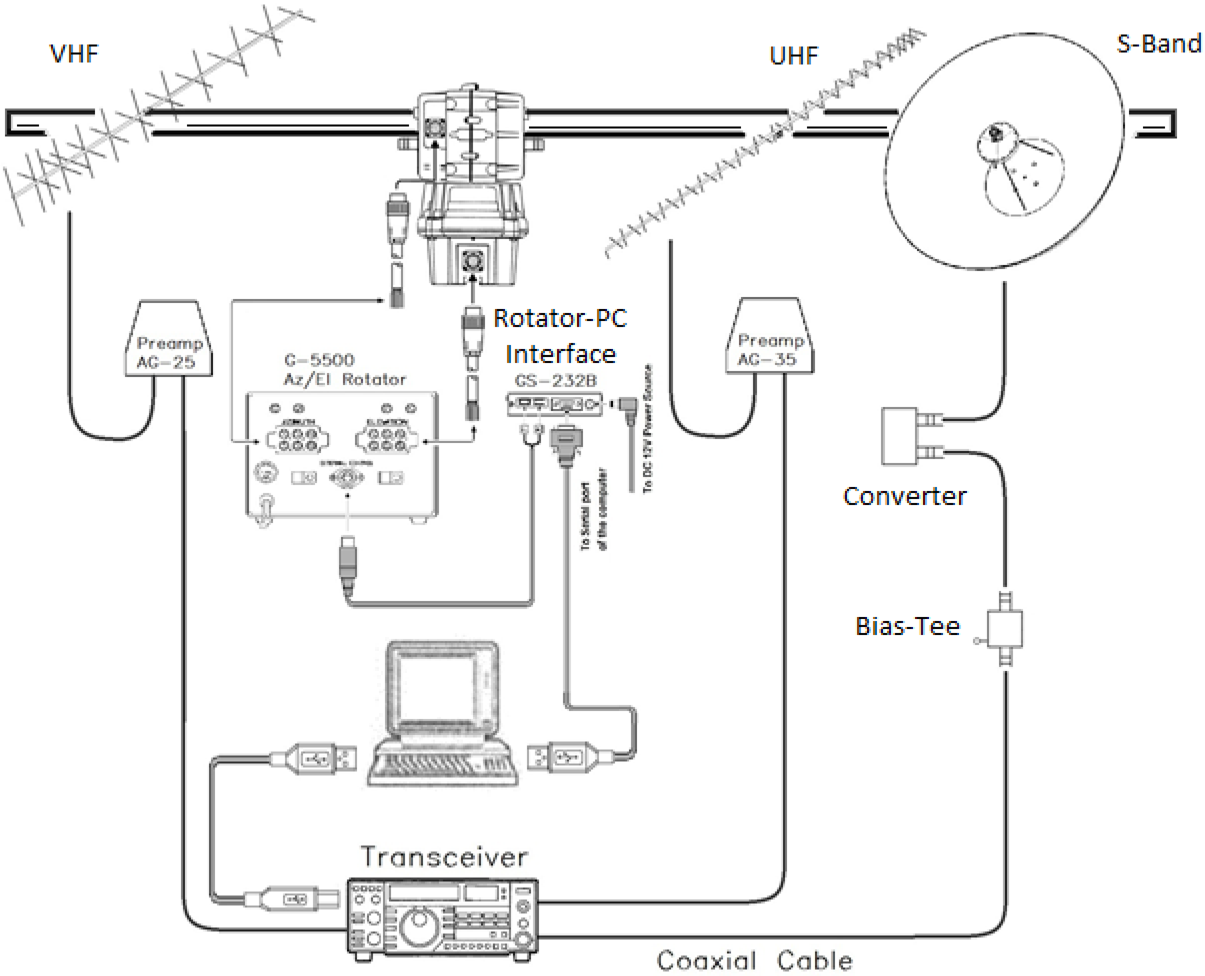

Fig. 30. The USYD ground station

Link budget for GAMALink

Table 14 shows the link budget for GAMALink.

Table 14. GAMALink link budget

System Design Parameters			Ground Link		ISL		
Frequency	Hz	f	2,45E+09		2,45E+09		Centre frequency
Maximum Distance	Km	d	1500		1000		Communications are designed for this limit
Bandwidth	Hz	BW	4,00E+07		4,00E+06		Bandwidth will determine noise power and signal redundancy
Transmission Power	W/d BW	C	3	4,77	3	4,77	RF power provided by the RF frontend

Data Rate	Kbps	R	1000		1000		Desired data rate
Environmental Parameters							
Reference Temperature	K	To	290	24,62	290	24,62	Temperature of the system
System Noise Temperature	K	Tsys	357,78	25,54	357,78	25,54	Noise temperature of the background
(-)10*LOG10(kTsys)			2,02E+20	203,06	2,02E+20	203,06	Inverse of noise power per Hz
Atmospheric Attenuation	dB/Km	Lg		-5		-5	Attenuation introduced by the atmosphere
Constants							
Boltzmann Constant	J/K	k	1,38E-23	-228,6	1,38E-23	-228,6	Universal constant
Speed of Light	m/s	c	3,00E+08		3,00E+08		Universal constant
Transmission							
Transmission Power	W/dBW	C	3	4,77	3	4,77	(RF power provided by the RF frontend)
Transmission Losses		Le	0,95	-0,22	0,95	-0,22	Losses from the RF frontend to the antenna
Transmission Gain		Ge	1,6	2,04	1,6	2,04	Transmission antenna gain
Misalignment Losses		Lp	0,5	-3,01	0,5	-3,01	Antenna misalignment losses
EIRP	W/dBW	EIRP	2,28	3,58	2,28	3,58	Irradiated power to receiver
Space Losses							
Free Space Losses (Friis Formula)		Lfs	4.22E-12	-163,75	9.49E-12	-160,23	Losses due to distance between transmitter and receiver
Polarization Losses			0,9	-0,46	0,9	-0,46	Losses due to polarization misalignment
Atmospheric Losses		Lag	0,31	-5,09	0,31	-5,09	Attenuation introduced by the atmosphere

Parabolic Dish Parameters							
Diameters	m	D	3			0,07	Effective diameter of the antenna
Total Efficiency		h	0,5	-3,01	0,5	-3,01	Efficiency of the antenna
Gain		Gr	2,962,1 10,017	34,72	1,612,7 04,343	2,08	Antenna gain
Noise Temperature	K	Tant	300			50	Noise temperature of the antenna
Reception							
Received Power Density	W/m 2		2.68E-13	-165,71	6.04E-12	-162,19	Signal power received at the antenna
Reception Gain		Gr	2,962,1 10,017	34,72	1,612,7 04,343	2,08	(Antenna gain)
Misalignment Losses			0,5	-3,01	0,5	-3,01	Receiving antenna misalignment
Reception Losses		Lr	0,9	-0,46	0,9	-0,46	Losses between antenna and RF frontend
Figure of Merit		G/T	4,443,1 65,025	6,48	0,01451 4339	-18,38	Figure of merit of receiving antenna
LNA Data							
Gain		Glna	100	20	40000	46,02	LNA gain
Receiver Sensitivity	W/d BW		1,00E-13	-130	1,00E-13	-130	Receiver sensitivity
Reception Data							
SNR		SNR	2,16E-01	-6,66	1,59E-02	-17,99	Signal to noise level at reception
Received Power	W/d bW		3.58E-07	-114,46	1.75E-07	-117,56	Signal power level at reception
Detectability			3,578,1 75	15,54	175,330 ,575	12,44	Relation of signal power level at reception to sensitivity
Data Rate							
Shannon Limit		Kbps	1,128,1 78,572		9,086,2 56,467		Theoretical maximal data rate
Spread spectrum code gain			128	21,07	1024	30,1	Gain introduced by coding symbols using orthogonal codes
QPSK Data Rate - 8 codes	Kbps		937,5		1,171,8 75		Data rate using codes

Code to Noise Ratio			2,763,736,423	14,41	1,625,077,017	12,11	Signal to noise ratio after correlation with codes
Bit Error Rate			3.70E-01		0,000442265		Bit error rate
1024 bit Packet Error Rate			0,003782366		0,05504927		Packet error rate without forward error correction
1024 bit PER with 1 bit FEC			7.16E-02		0,00153197		Packet error rate with 1 bit forward error correction
1024 bit PER with 2 bits FEC			9.02E-04		2.83E+00		Packet error rate with 2 bits forward error correction

Link budget for ISIS transceiver

Table 15 and 16 show the link budget for the ISIS transceiver.

Table 15 Uplink budget

Gereral Information			
Transmitter at	Ground Station	Receiver at	i-INSPIRE II
Orbit Altitude	350km	Elevation Angle	30°
Slant Range	652.5km	Weather	Clear Sky
Demodulation Method	AFSK	Cable Length	20m
Antenna Type(Tx)	Cross Yagi	Antenna Type(Rx)	Diople

Transmitter System (at Ground Station)		
Ground Station Transmitter Power Output	100	W
	20	dBW
Ground Station Total Transmission Line Losses	3.4	dB
Ground Station Antenna Gain	18.9	dBi
Ground Station ERIP	35.5	dBW
Down Link Path		
Free-Space Path Loss	132	dB
Satellite Antenna Pointing Loss (10°)	10.6	dB
Ground Station Antenna Pointing Loss (10°)	2.7	dB
Satellite Transmission Line Losses	0.5	dB
Atmospheric Loss (30°)	0.4	dB
Ionospheric Loss	0.4	dB
Rain Loss	0	dB
Total Loss	146.6	dB
Receiver System (at i-INSPIRE II)		
Antenna Gain	2.7	dBi
Effective Noise Temperature at Space (350km/Day)	1345	K
Figure of Merrit (G/T_s)	-28.6	dB/K
Carrier-to-Thermal-Noise Ratio (C/T)	-136.6	dB
Boltzmann's constant (K)	-228.6	dBW/K/Hz
Carrier-to-Noise Density Ratio C/N_o	88.9	dBHz
Modulation Process		
System Desired Data Rate	1200	pbs
Demodulation Method Seleted	AFSK	
System Allowed or Specified Bit-Error-Rate	10E-5	
Demodulator Implementation Loss	2	dB
Link Performance		
Required E_b/N_o	56.1	dB
Threshold E_b/N_o	23.2	dB
System Link Margin*	**32.9**	**dB**

*This value must be great 0.0 dB for the link to work or close. A target value should be greater than 10 dB

Table 16 Downlink budget

Gereral Information			
Transmitter at	i-INSPIRE II	Receiver at	Ground Station
Orbit Altitude	350km	Elevation Angle	30°
Slant Range	652.5km	Weather	Clear Sky
Demodulation Method	BPSK	Cable Length	20m
Antenna Type(Tx)	Diople	Antenna Type(Rx)	Cross Yagi

Transmitter System (at i-INSPIRE II)		
Satellite Transmitter Power Output	0.5	W
	-3.01	dBW
Satellite Total Transmission Line Losses	0.5	dB
Satellite Antenna Gain	2.7	dBi
Satellite ERIP	-0.81	dBW

Down Link Path		
Free-Space Path Loss	132	dB
Satellite Antenna Pointing Loss (10°)	10.6	dB
Ground Station Antenna Pointing Loss (10°)	0.8	dB
Ground Station Transmission Line Losses	1.8	dB
Atmospheric Loss (30°)	0.4	dB
Ionospheric Loss	0.8	dB
Rain Loss	0	dB
Total Loss	146.4	dB

Receiver System (at Ground Station)		
Antenna Gain	14.4	dBi
Effective Noise Temperature at Sydney (SL/Day)	610.1	K
Figure of Merrit (G/T_s)	-13.5	dB/K
Carrier-to-Thermal-Noise Ratio (C/T)	-160.71	dB
Boltzmann's constant (K)	-228.6	dBW/K/Hz
Carrier-to-Noise Density Ratio C/N_o	67.89	dBHz

Modulation Process		
System Desired Data Rate	9600	pbs
Demodulation Method Seleted	BPSK	
System Allowed or Specified Bit-Error-Rate	10E-5	
Demodulator Implementation Loss	2	dB

Link Performance		
Required E_b/N_o	26.07	dB
Threshold E_b/N_o	10.5	dB
System Link Margin*	**15.56**	**dB**

*This value must be great 0.0 dB for the link to work or close.
A target value should be greater than 10 dB